

# Computation of fiber orientation in X-ray micro-tomography reconstructions

Presented by Federico Semeraro  
Monday 16<sup>th</sup> September 2019

Authors: Federico Semeraro<sup>1</sup>, Joseph C. Ferguson<sup>1</sup>,  
Francesco Panerai<sup>2</sup>, Nagi N. Mansour<sup>3</sup>

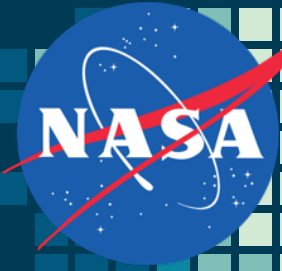
1. Science and Technology Corp. at NASA Ames Research Center, Moffett Field, CA 94035
2. Department of Aerospace Engineering, University of Illinois at Urbana-Champaign, IL 61801
3. NASA Ames Research Center, Mail Stop 258-5, Moffett Field, CA 94035

Technical Session #1:  
Micro-tomography based analysis



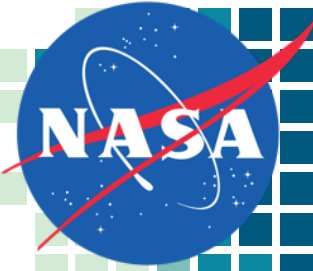
Ablation Workshop





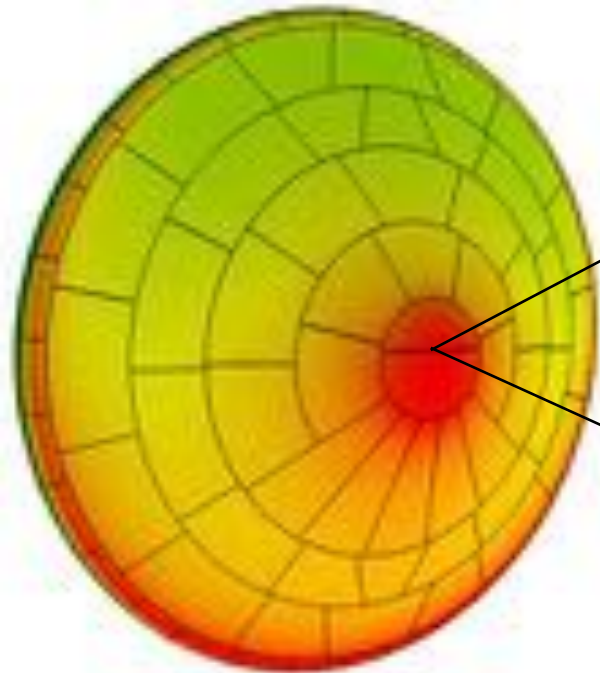
# MOTIVATION & OBJECTIVES

# Modeling Thermal Protection Systems (TPS)



## Macroscale Modeling

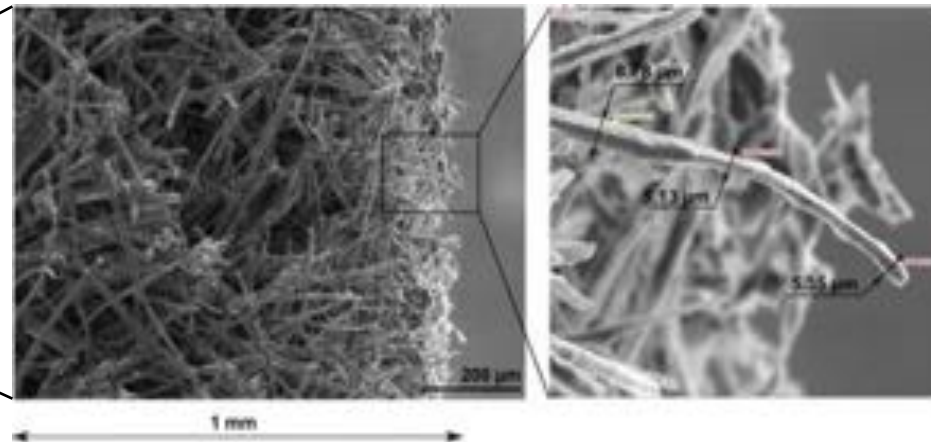
Full scale material response solvers, using volume-averaged techniques to solve conservation equations for ablation



Simulation of surface temperature for MSL heatshield\*<sup>1</sup>

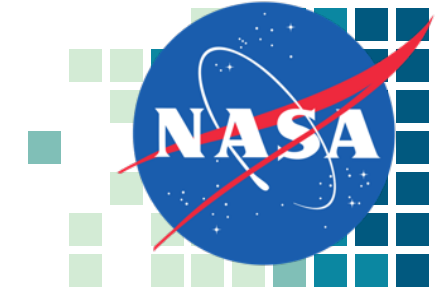
## Microscale Modeling

Used to inform material properties and material response parameters used in macro-scale modeling

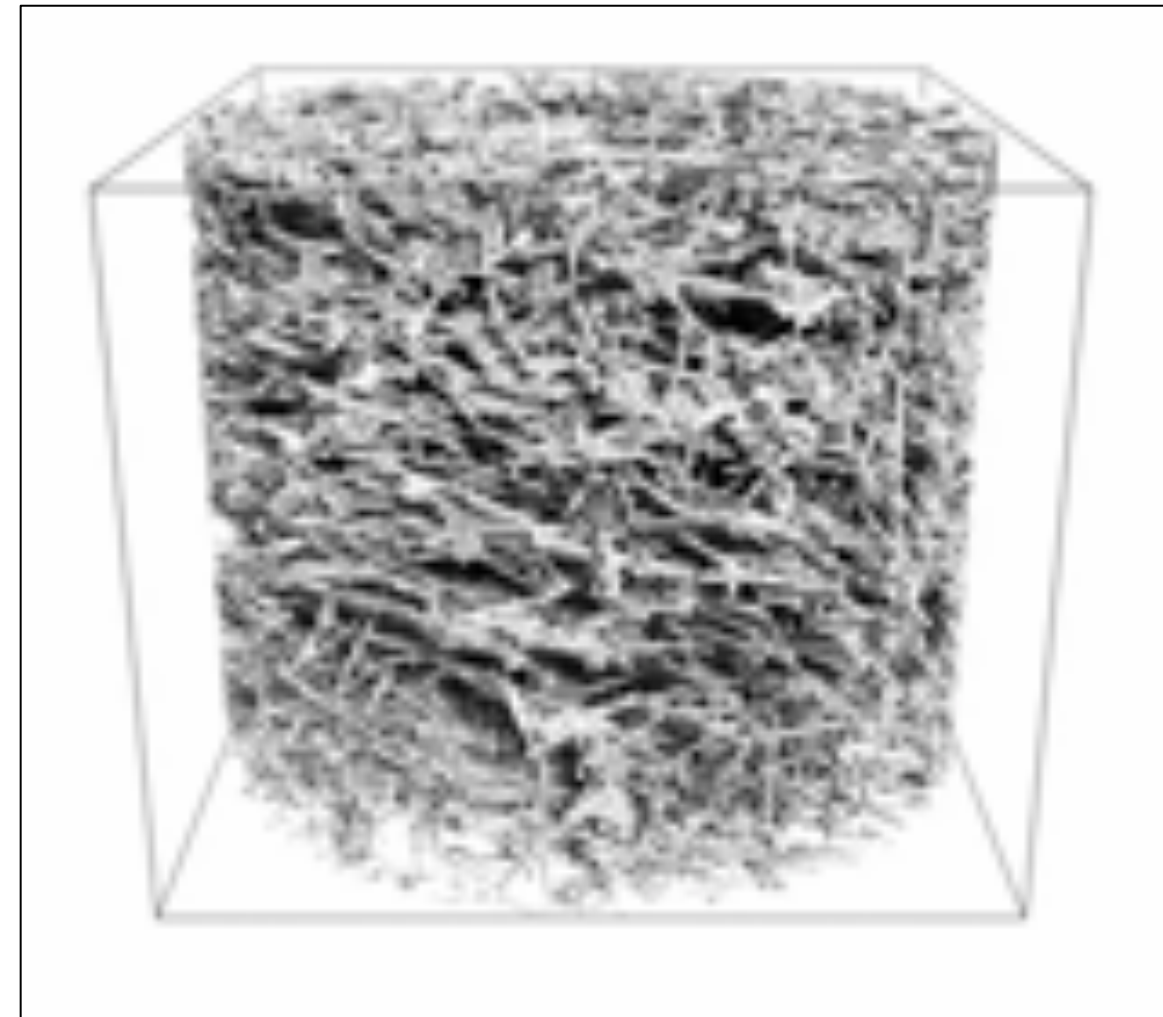
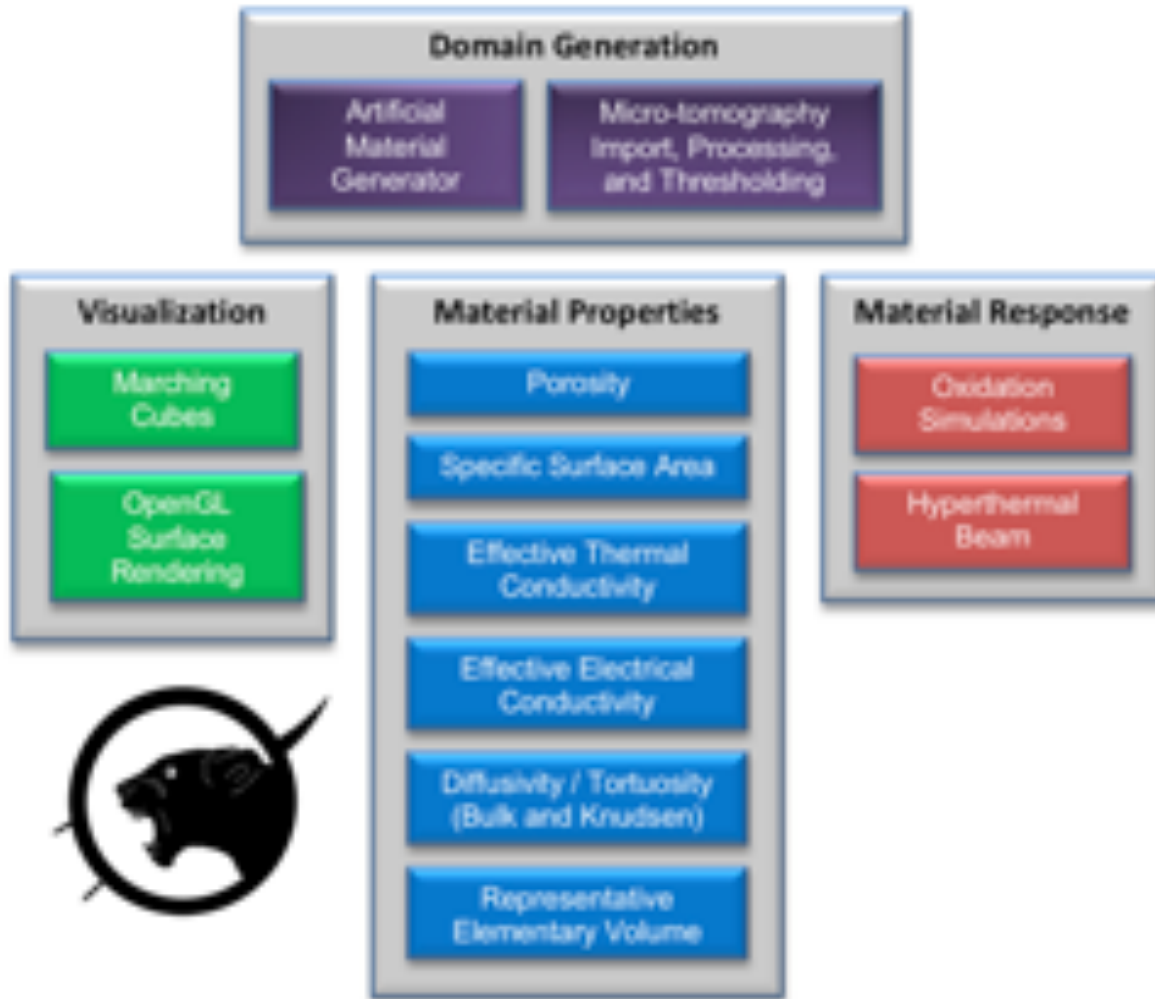


Lachaud and Mansour, *JTHT* 2013

\*<sup>1</sup> Meurisse, Jeremie BE, et al. "Multidimensional material response simulations of a full-scale tiled ablative heatshield." *Aerospace Science and Technology* 76 (2018): 497-511.



# Porous Microstructure Analysis (PuMA)

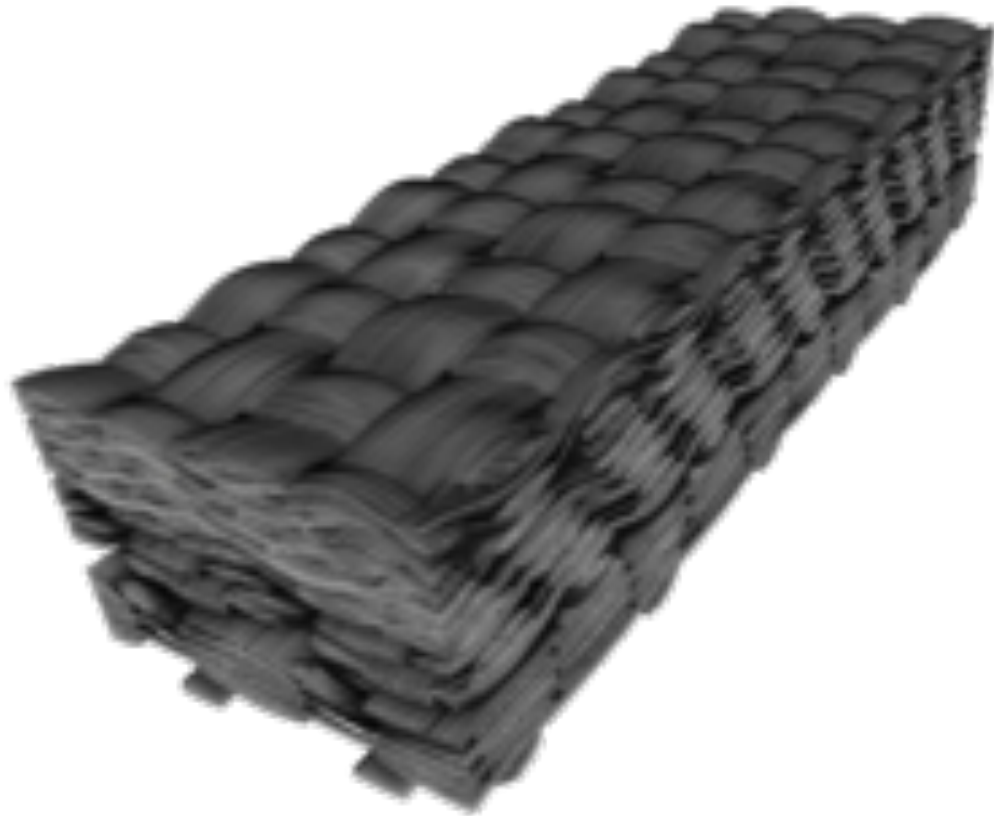
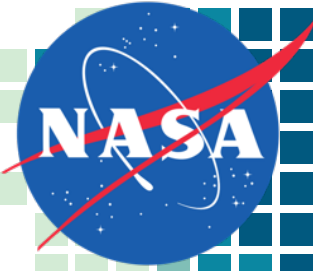


CT Reconstruction of FiberForm

Ferguson, J. C., Panerai, F., Borner, A., & Mansour, N. N. (2018). PuMA: the Porous Microstructure Analysis software. *SoftwareX*, 7, 81-87.

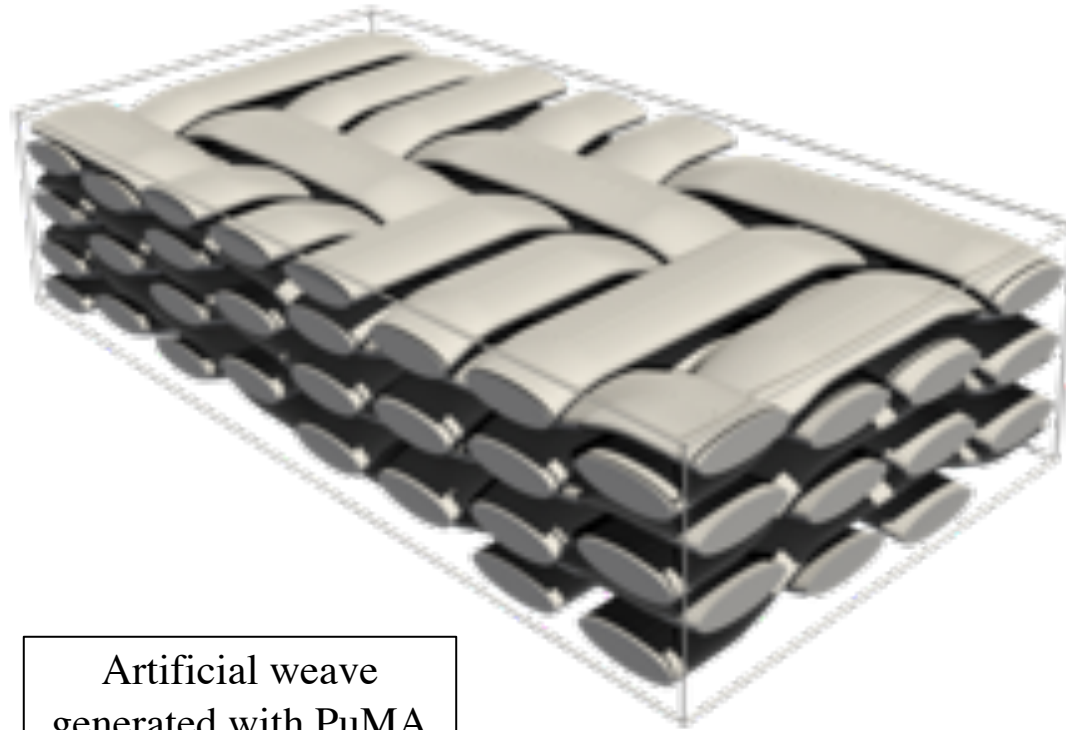
<https://software.nasa.gov/software/ARC-17920-1>

# Challenges in Micro-scale modeling



12-ply real  
TPS weave

As NASA moves towards  
woven TPS materials, our  
modeling must adapt

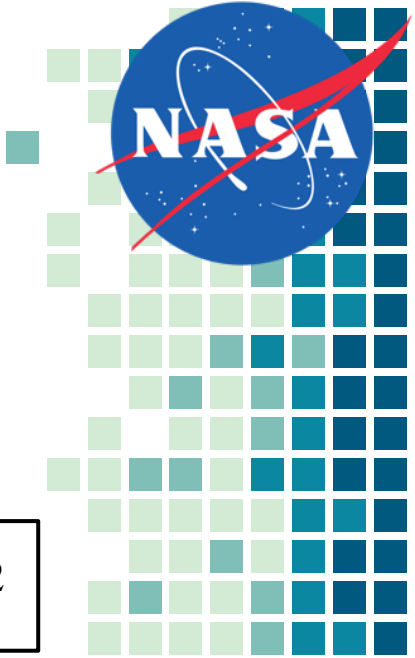


Artificial weave  
generated with PuMA



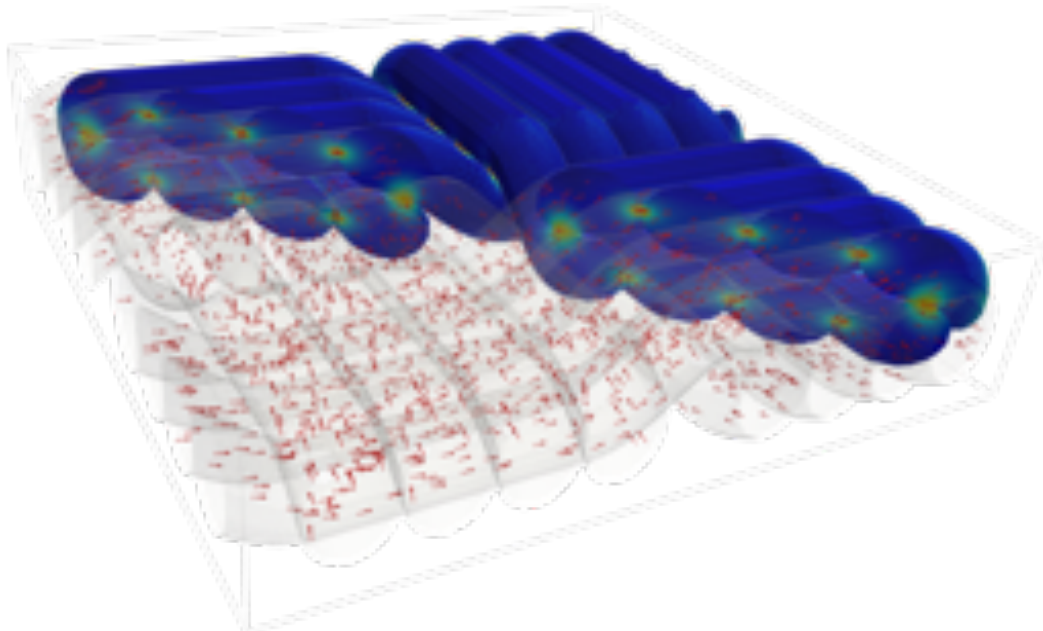


# Objectives

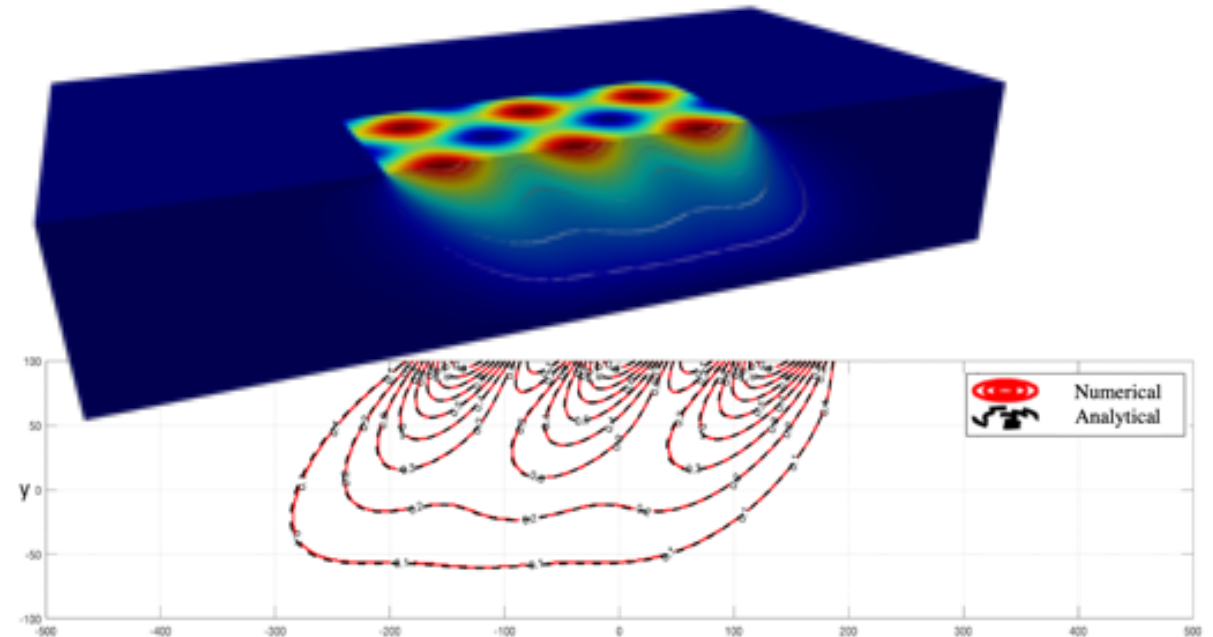


Computation of Effective Material Properties

Fiber Orientation Estimation\*<sup>1</sup>

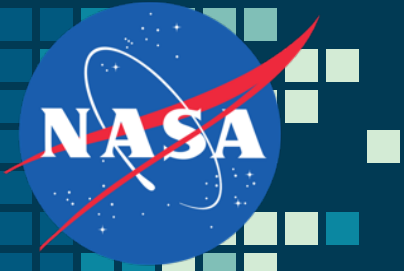


Physical and Numerical Model\*<sup>2</sup>

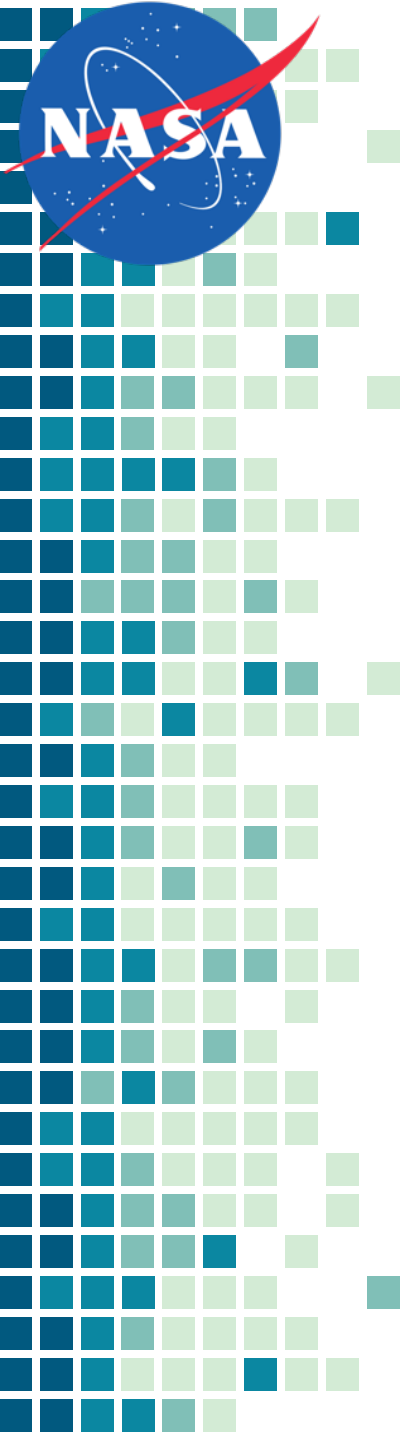


\*<sup>1</sup> Federico Semeraro, Joseph C. Ferguson, Francesco Panerai, Robert J. King, Nagi N. Mansour. Anisotropic Analysis of Fibrous and Woven Porous Media, Part I: Estimation of Local Material Orientation. *Journal of Computational Physics* [to appear]

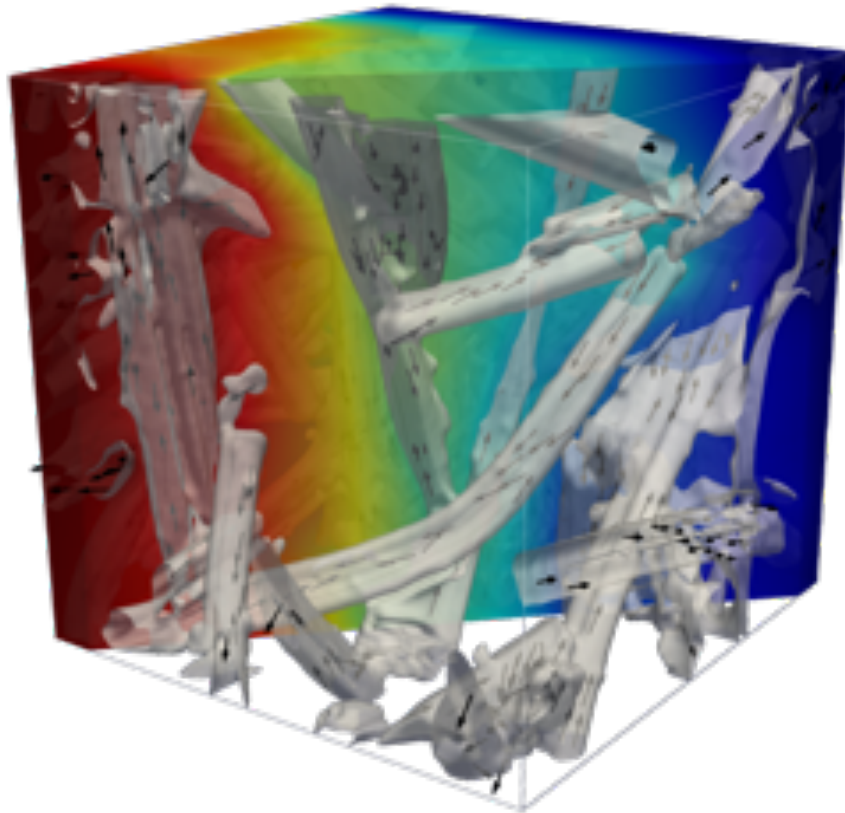
\*<sup>2</sup> Federico Semeraro, Joseph C. Ferguson, Francesco Panerai, Nagi N. Mansour. Anisotropic Analysis of Fibrous and Woven Porous Media, Part II: Computation of Effective Conductivity. *Journal of Computational Physics* [to appear]



# FIBER ORIENTATION METHODS



# Overview

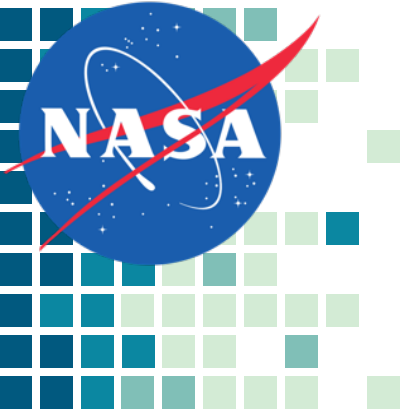


- Ray Casting (novel)
- Artificial Flux\*<sup>1</sup>
- Structure Tensor\*<sup>2</sup>

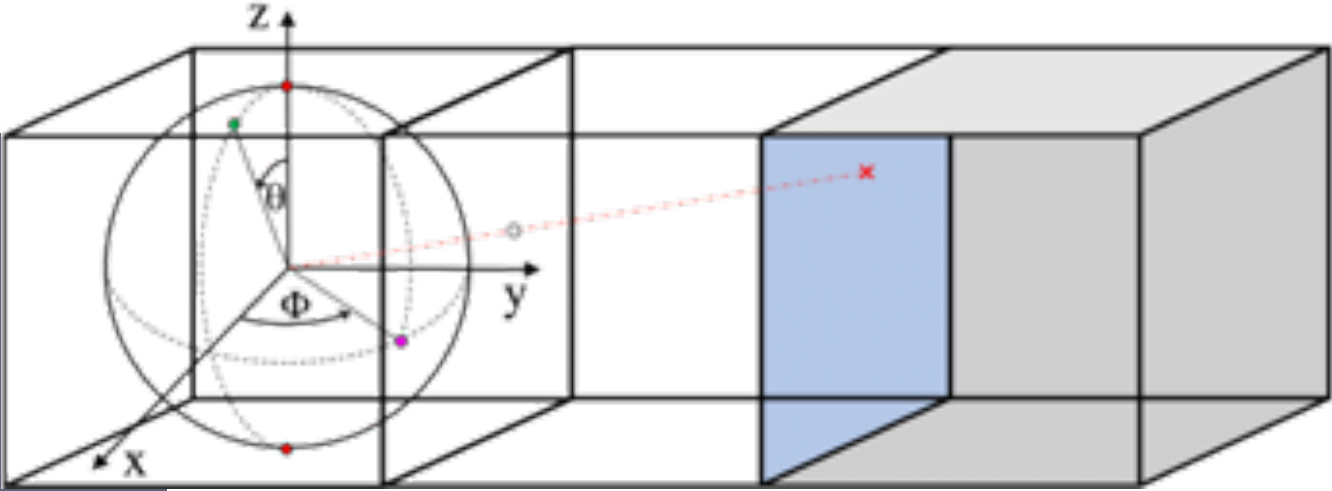
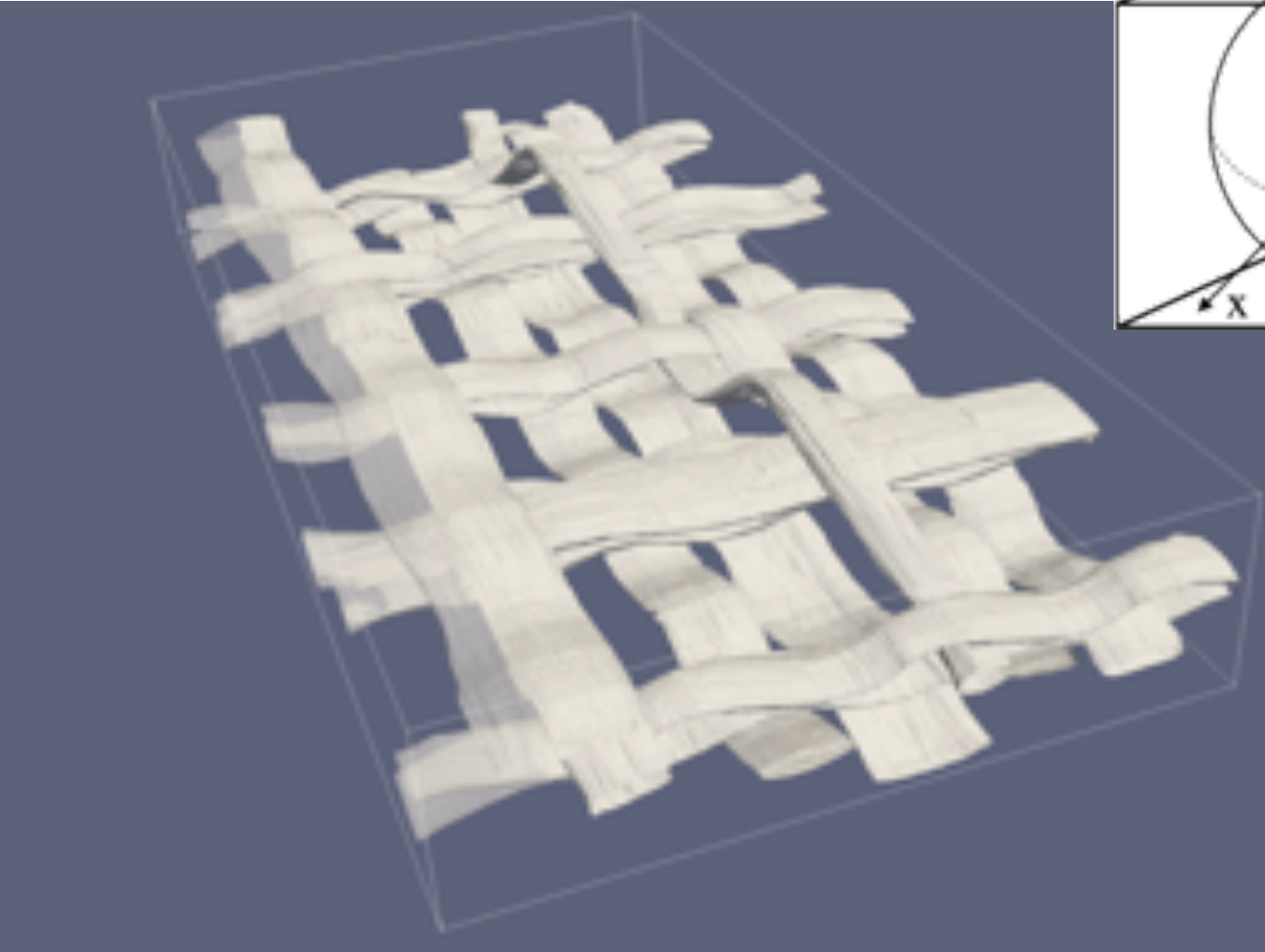
\*<sup>1</sup> Matti Schneider, Matthias Kabel, Heiko Andrä, et al. Thermal fiber orientation tensors for digital paper physics. *International Journal of Solids and Structures* 2016; 100-101 234

\*<sup>2</sup> Krause M, Hausherr JM, Burgeth B, Herrmann C, Krenkel W. Determination of the fibre orientation in composites using the structure tensor and local x-ray transform. *J Mater Sci* 2010; 45(4):888–96.



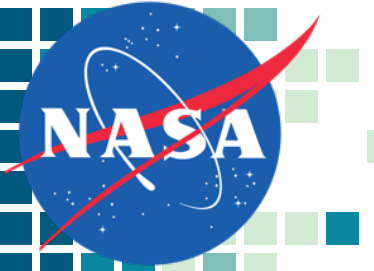


# Ray Casting

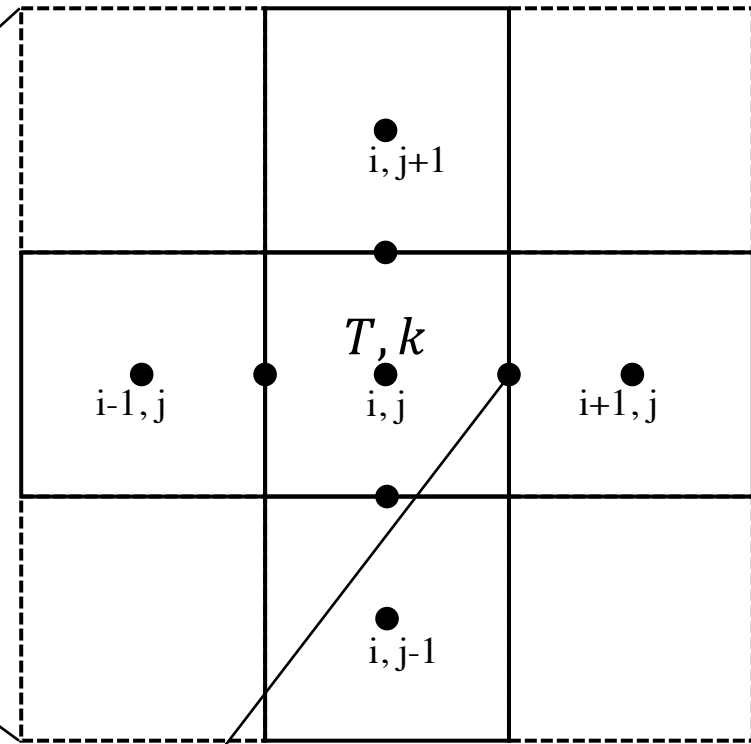
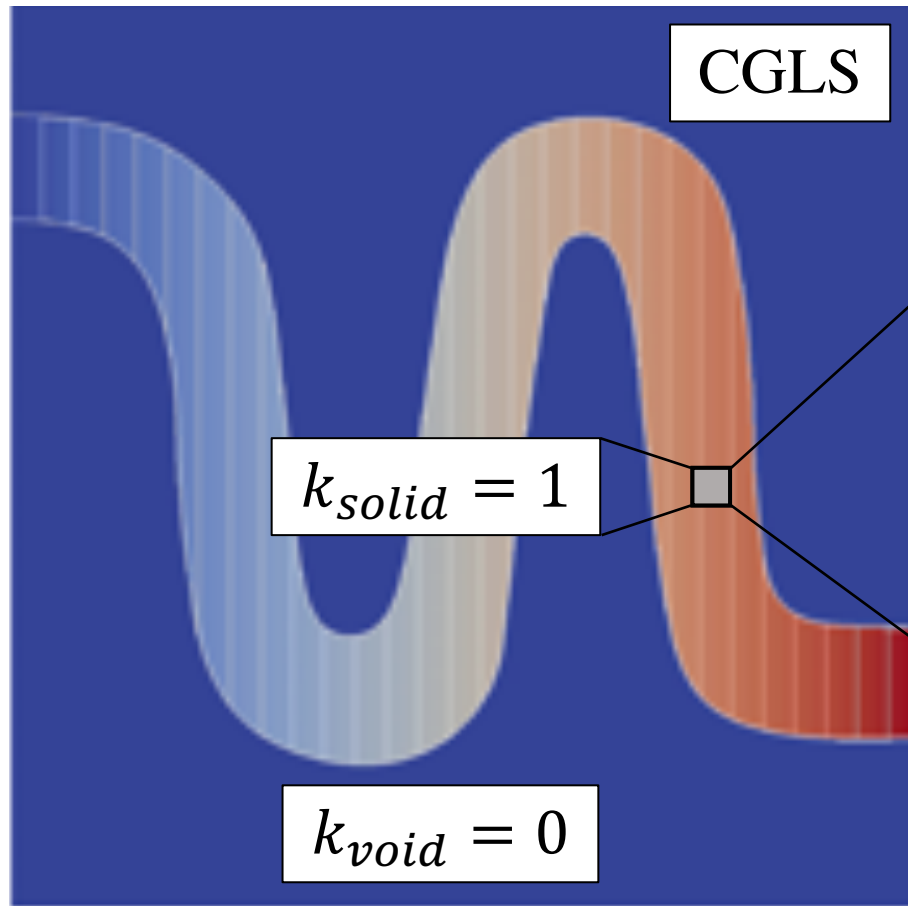


$$\theta \in [0, 180^\circ) \quad \phi \in [0, 360^\circ)$$

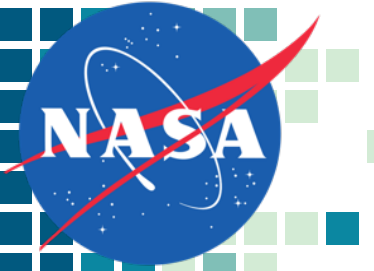
$$N = \left( \frac{180^\circ}{d\psi} - 1 \right) \left( \frac{360^\circ}{d\psi} \right) + 2$$



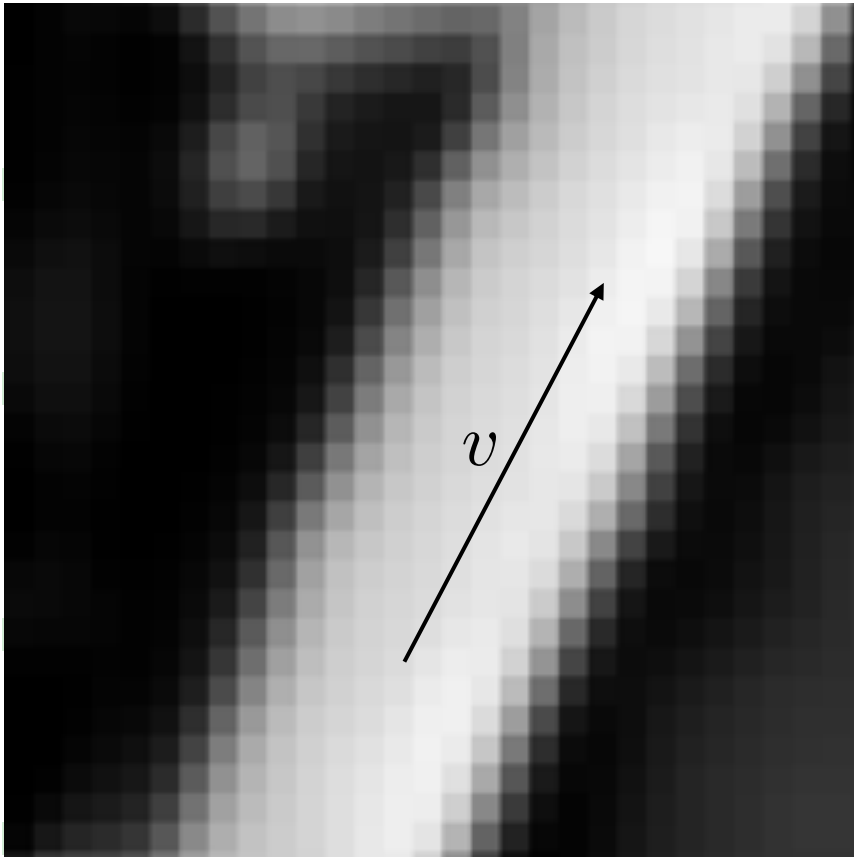
# Artificial Flux



$$T_{i+1/2} = \frac{k_{i+1}}{k_i + k_{i+1}} T_{i+1} + \frac{k_i}{k_i + k_{i+1}} T_i$$



# Structure Tensor



$$(I(x + v) - I(x))^2 \approx 0$$

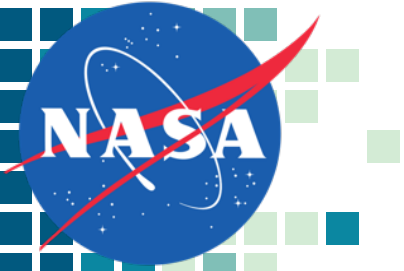
4 Steps:

1.  $\nabla I_\sigma(x) = \nabla(\sigma * I(x))$

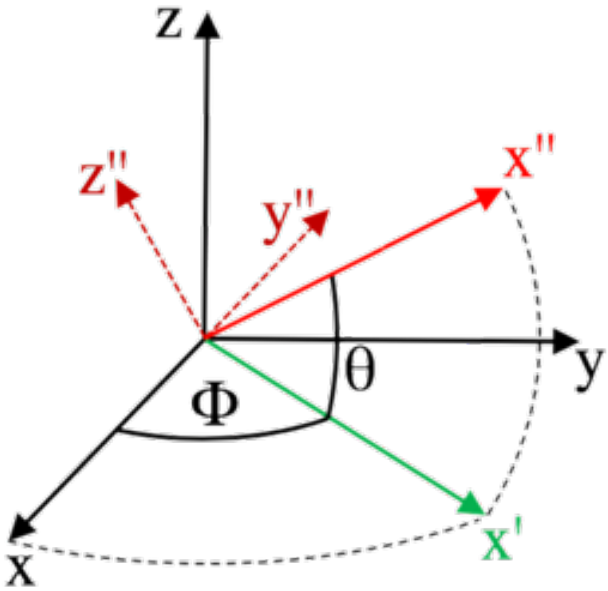
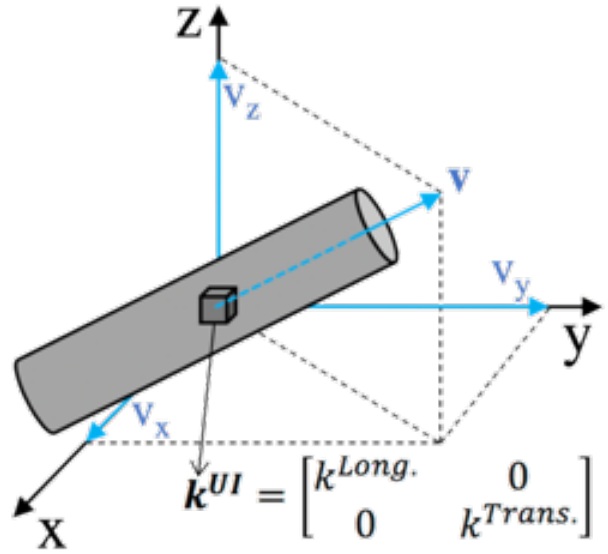
2. 
$$\nabla I_\sigma \nabla I_\sigma^T = \begin{pmatrix} I_x^2 & I_x I_y & I_x I_z \\ I_x I_y & I_y^2 & I_y I_z \\ I_x I_z & I_y I_z & I_z^2 \end{pmatrix}$$

3.  $J_\rho(x) = \rho * (\nabla I_\sigma \nabla I_\sigma^T)$

4. Local orientation vector  $v$  is the eigenvector related to the smallest eigenvalue of  $J_\rho(x)$



# Conductivity Tensor Rotation



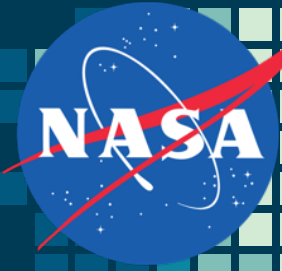
$$\mathbf{v} = v_x \mathbf{i} + v_y \mathbf{j} + v_z \mathbf{k}$$

$$\mathbf{k}'' = \begin{bmatrix} k^{Long.} & 0 & 0 \\ 0 & k^{Trans.} & 0 \\ 0 & 0 & k^{Trans.} \end{bmatrix}$$

$$\theta = \arcsin v_z \quad \phi = \arctan \frac{v_y}{v_x}$$

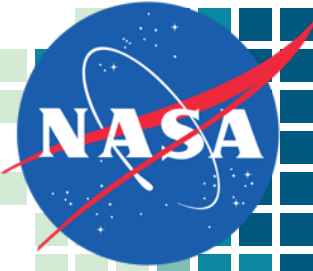
$$\mathbf{q} = \underbrace{[\mathbf{R}^{-1} \mathbf{k}'' \mathbf{R}]}_{\mathbf{k}} \nabla T$$

$$\mathbf{R} = \begin{bmatrix} \cos \theta & 0 & -\sin \theta \\ 0 & 1 & 0 \\ \sin \theta & 0 & \cos \theta \end{bmatrix} \begin{bmatrix} \cos \phi & \sin \phi & 0 \\ -\sin \phi & \cos \phi & 0 \\ 0 & 0 & 1 \end{bmatrix}$$



# APPLICATION TO MATERIALS

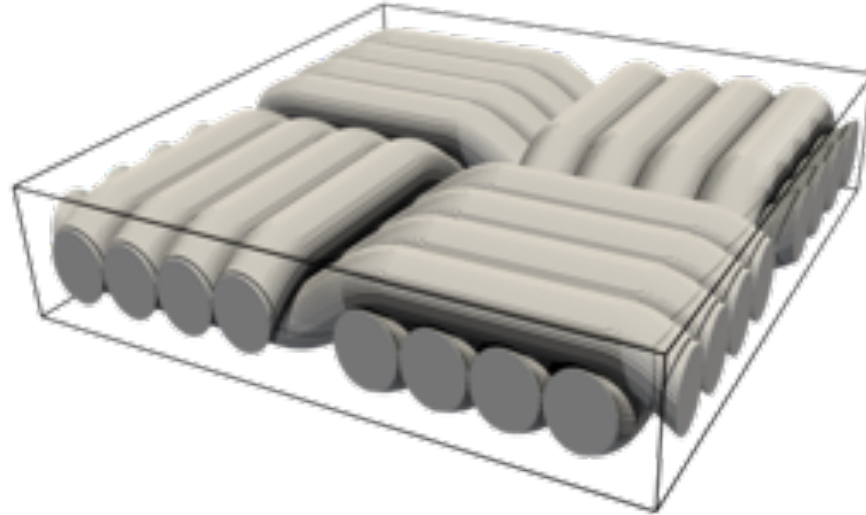
# Parametric Study



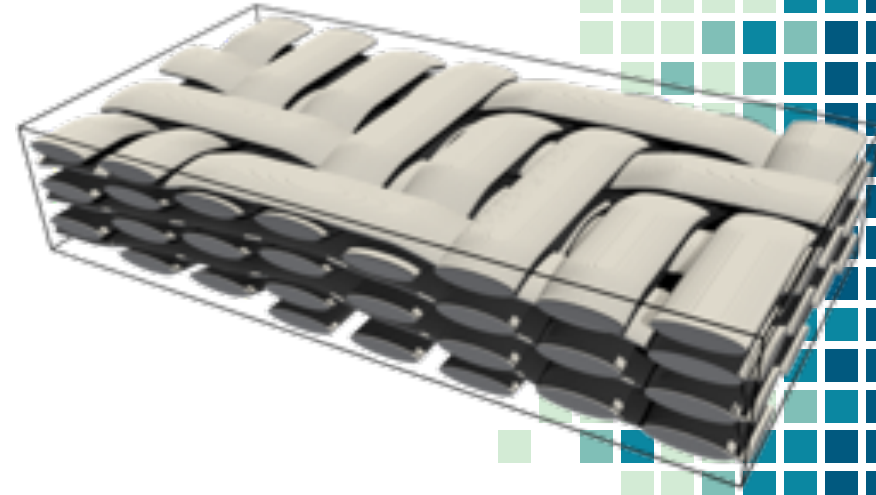
Artificial Straight Fibers



2D Weave



3D Weave



## Methods' Inputs

Ray Casting (RC)

~~Ray angle  
separation  $d\psi$~~

Artificial Flux (AF)

~~Solver Tolerance~~

Structure tensor (ST)

Kernel window sizes:

1.  $\sigma$
2.  $\rho$

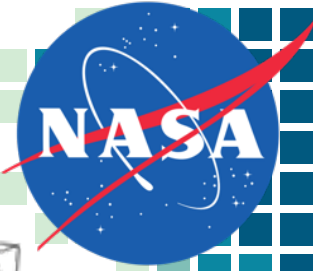
## Methods' Performance

Mean Angular Error

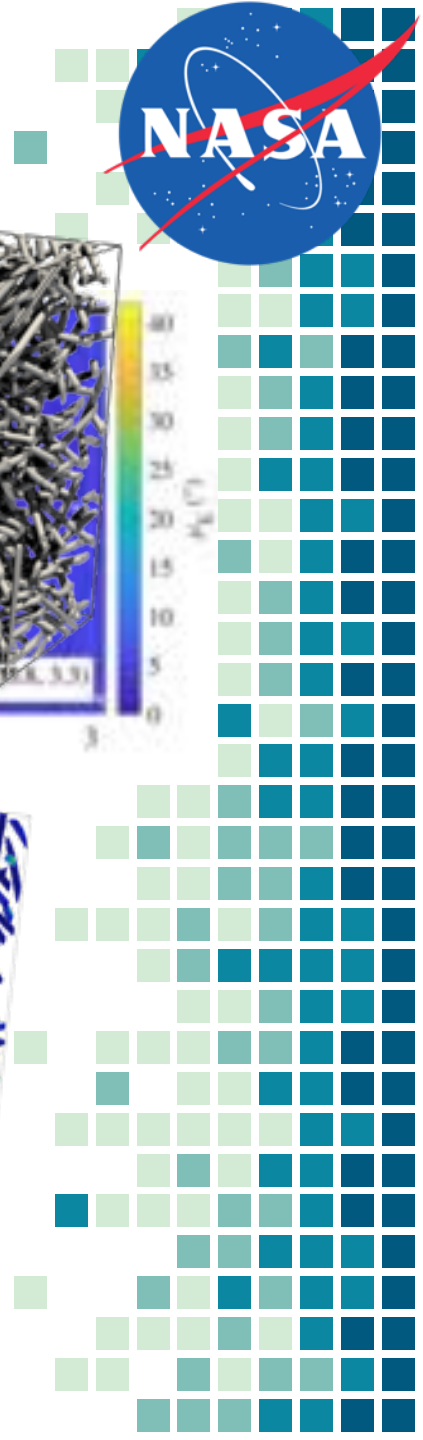
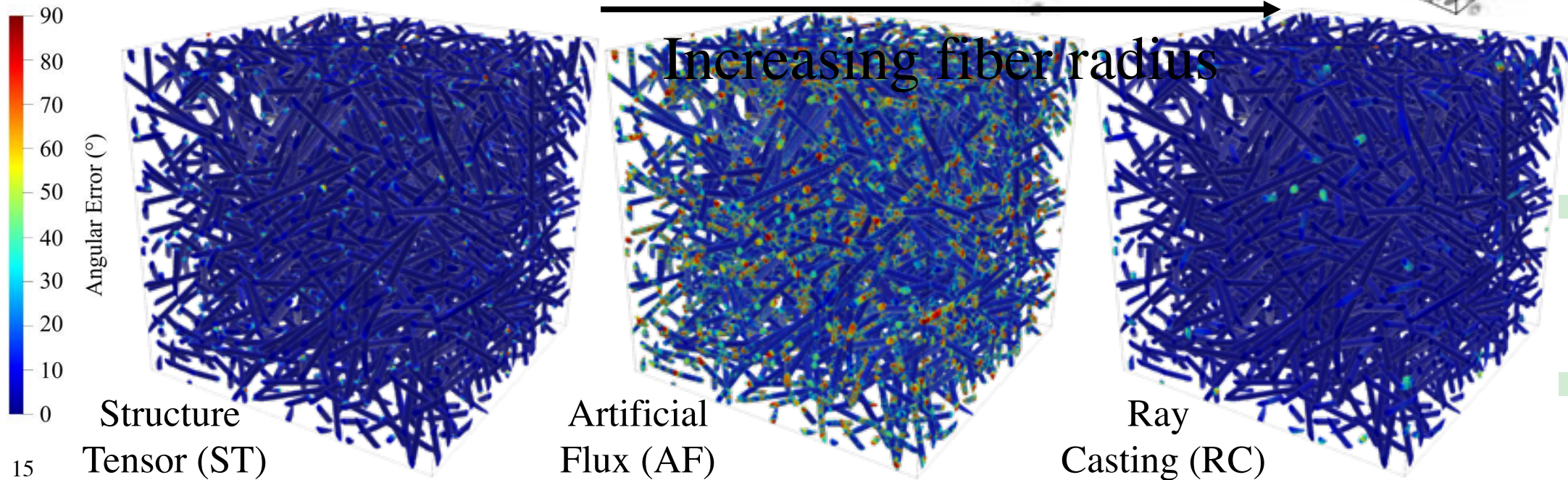
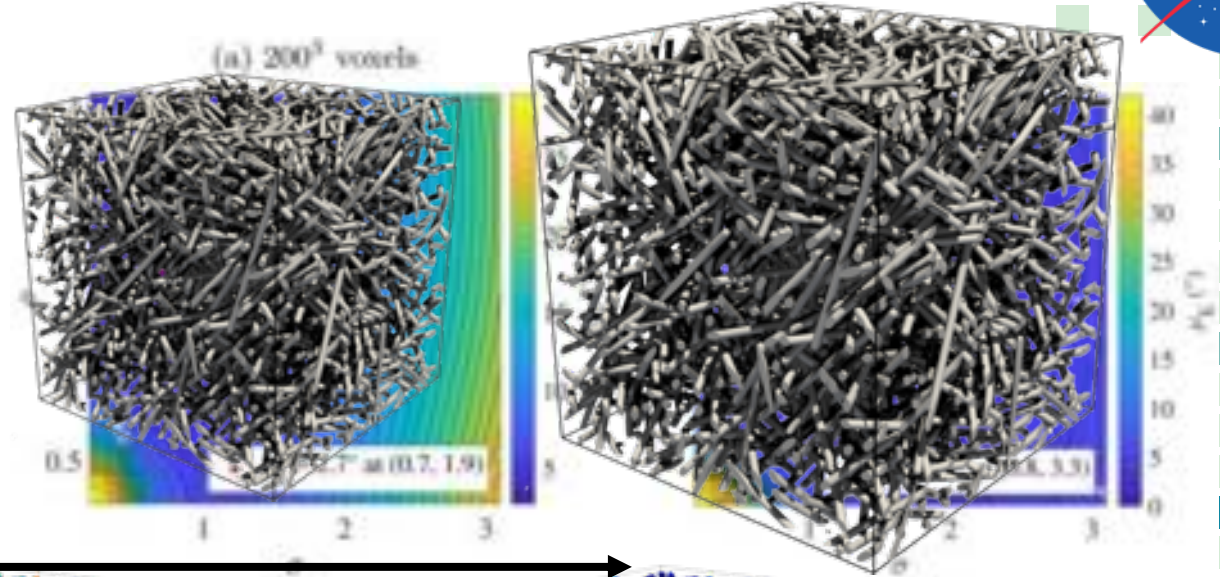
$$\mu_E = \sum_{n=1}^{N_{solid}} \frac{\alpha_n(x)}{N_{solid}}$$



# Results on Artificial Fibrous Samples

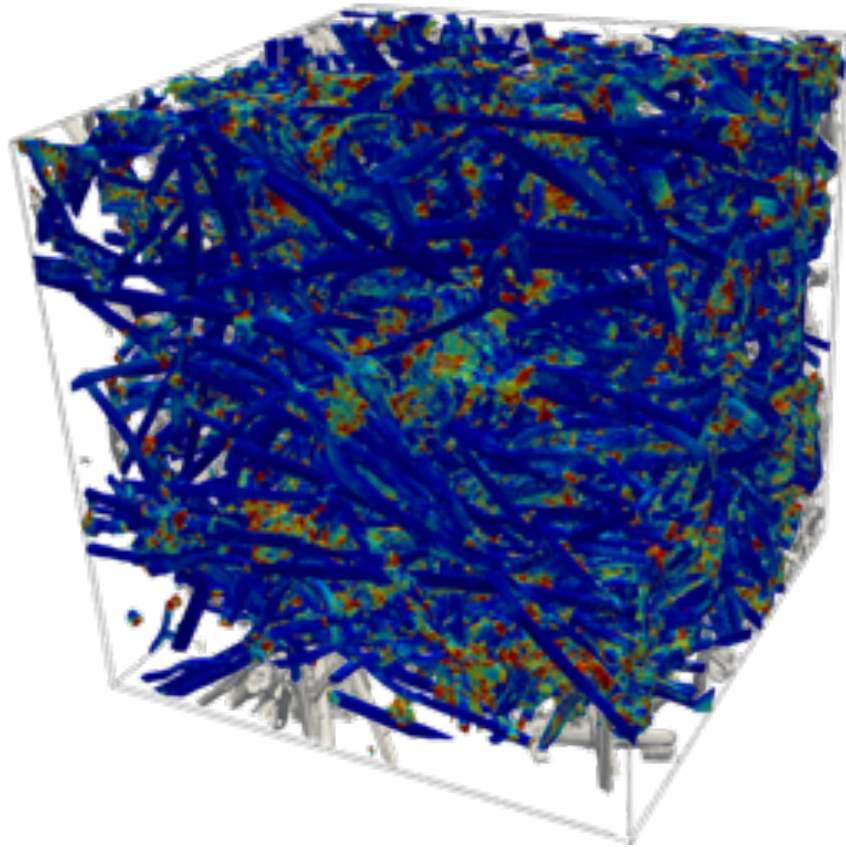
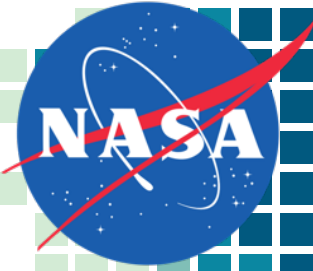


Resolution (vox)	$\mu_{E,ST}(\text{°})$	$\mu_{E,AF}$	$\mu_{E,RC}$
$200^3$	20.5	20.5	20.5
$400^3$	17.3	17.3	17.3
$600^3$	16.7	16.7	16.7
$800^3$	1.8	16.7	16.2



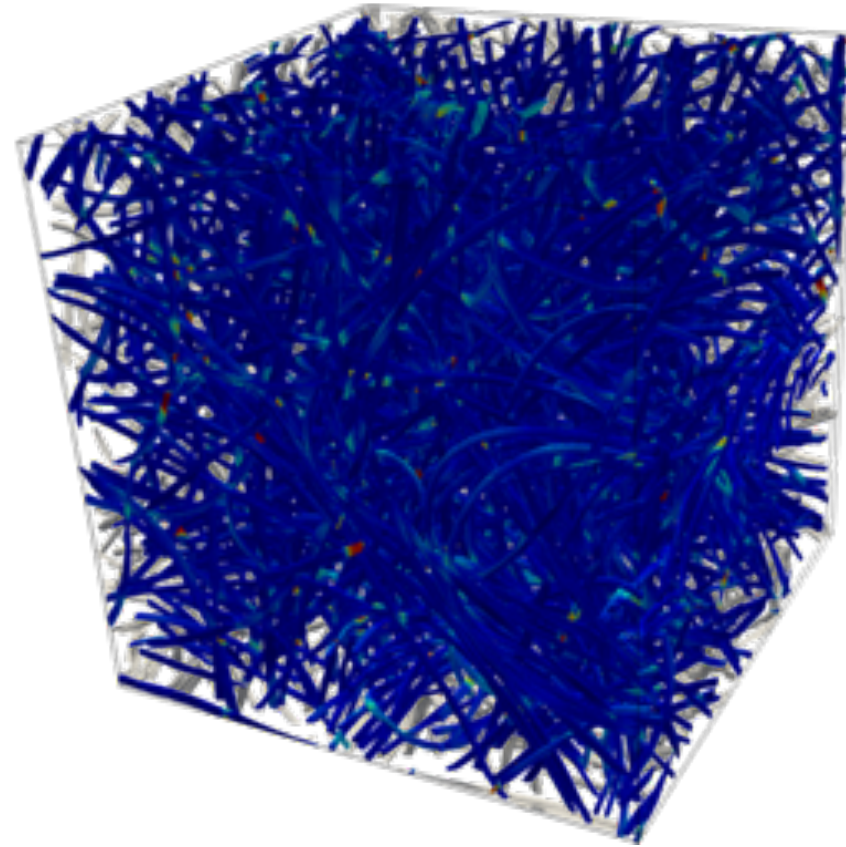
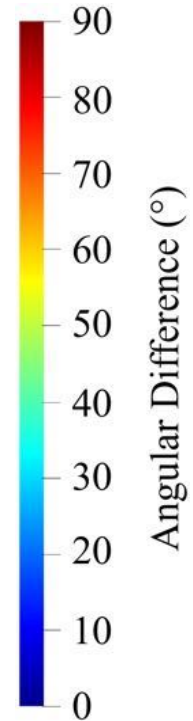


# Results on Real Fibrous Samples



FiberForm™ 800<sup>3</sup> voxels

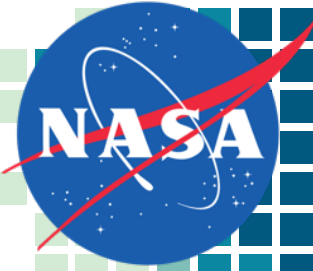
$$\mu_{\alpha} = 21.6^{\circ}$$



Morgan Felt 800<sup>3</sup> voxels

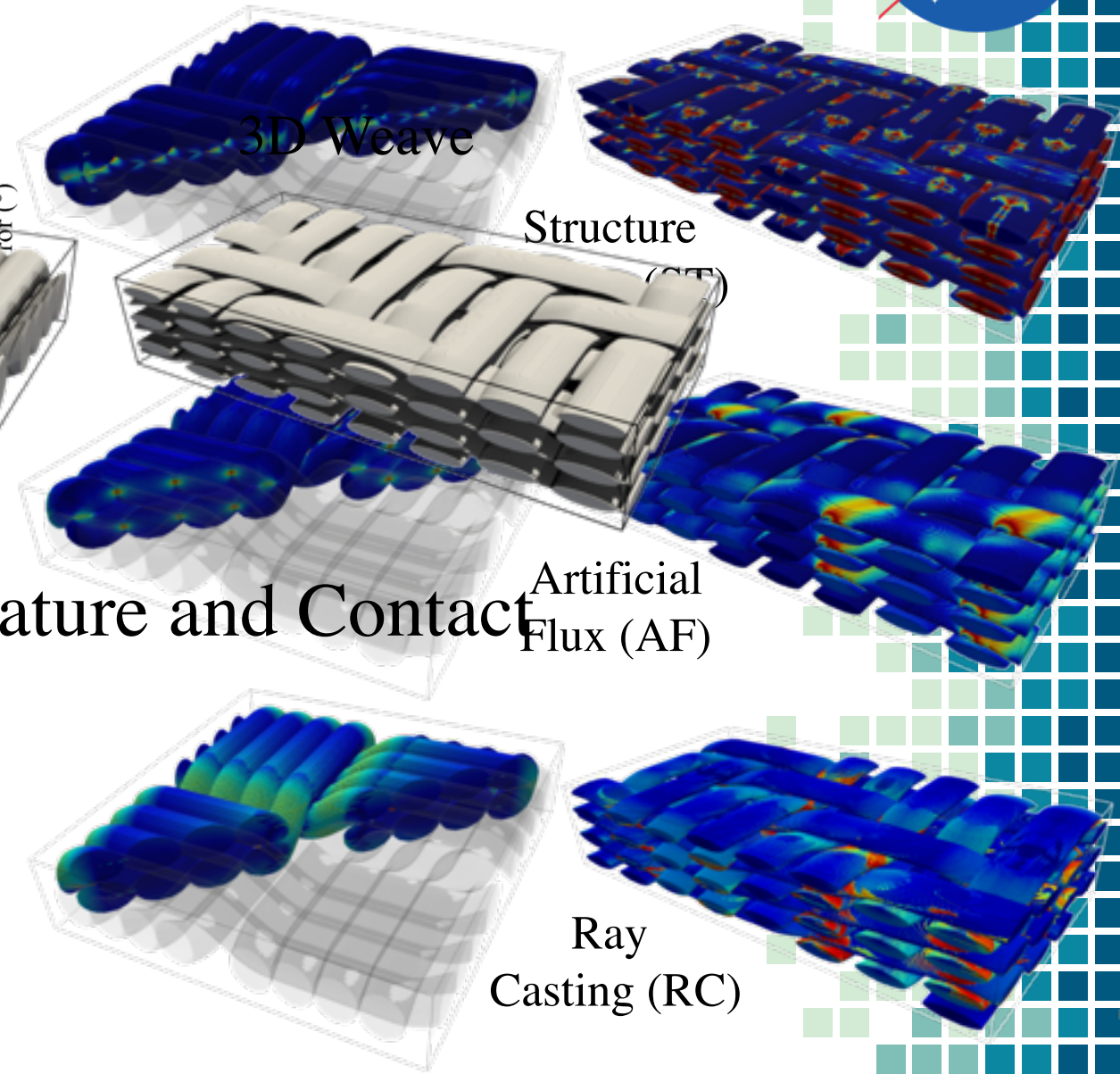
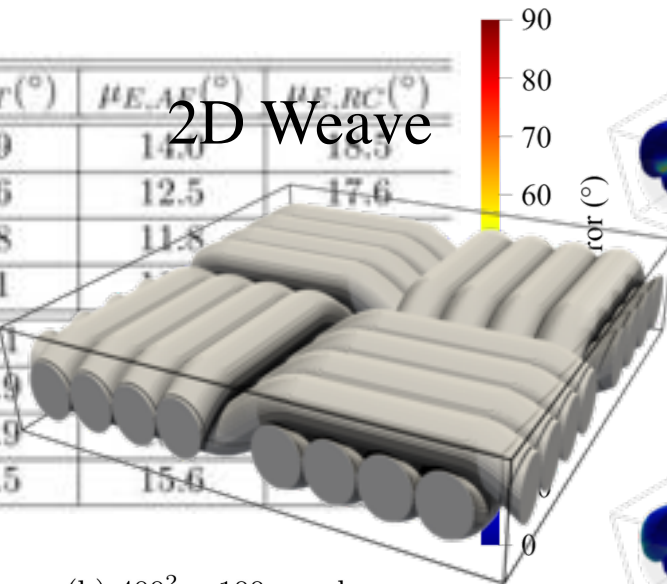
$$\mu_{\alpha} = 8.5^{\circ}$$

Structure Tensor  
v.s.  
Ray Casting



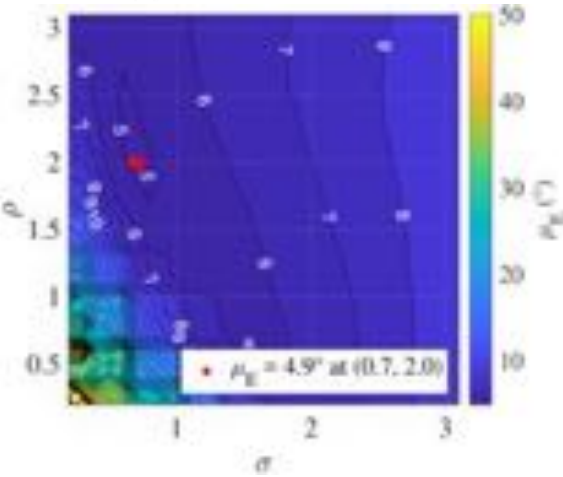
# Results on Artificial Woven Samples

Design	Resolution (vox)	$\mu_{E,ST}(\circ)$	$\mu_{E,AF}(\circ)$	$\mu_{E,RC}(\circ)$
Circular Tows	$200^2 \times 50$	4.9	14.0	18.5
	$400^2 \times 100$	4.6	12.5	17.6
	$600^2 \times 150$	4.8	11.8	
	$800^2 \times 200$	5.1		
Elliptical Tows	$200 \times 400 \times 80$	30.1		
	$400 \times 800 \times 160$	25.9		
	$600 \times 1200 \times 240$	25.9		
	$800 \times 1600 \times 320$	26.5	15.6	

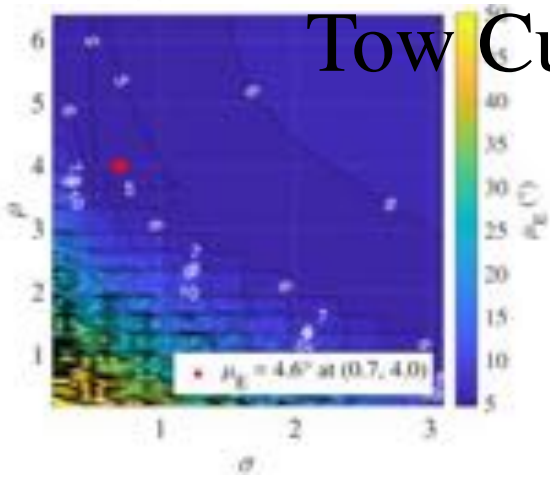


## Tow Curvature and Contact

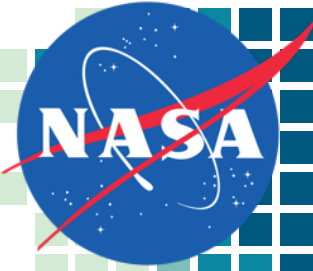
(a)  $200^2 \times 50$  voxels



(b)  $400^2 \times 100$  voxels

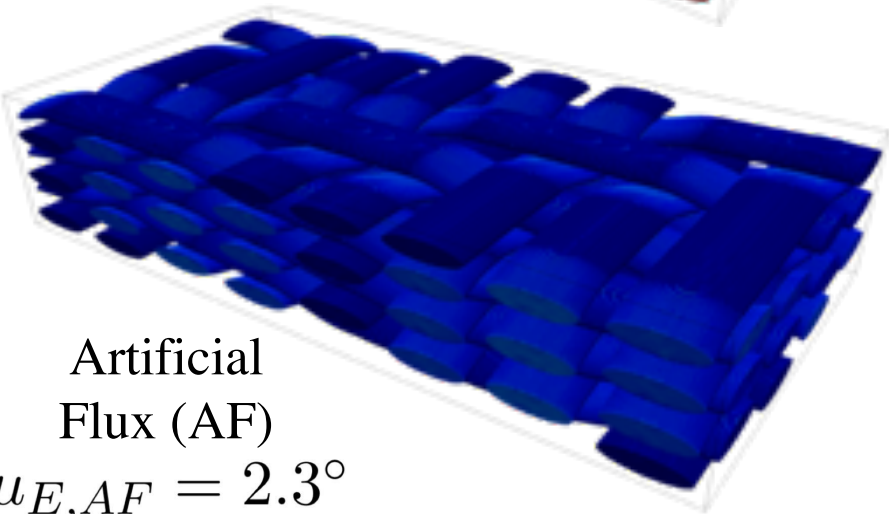
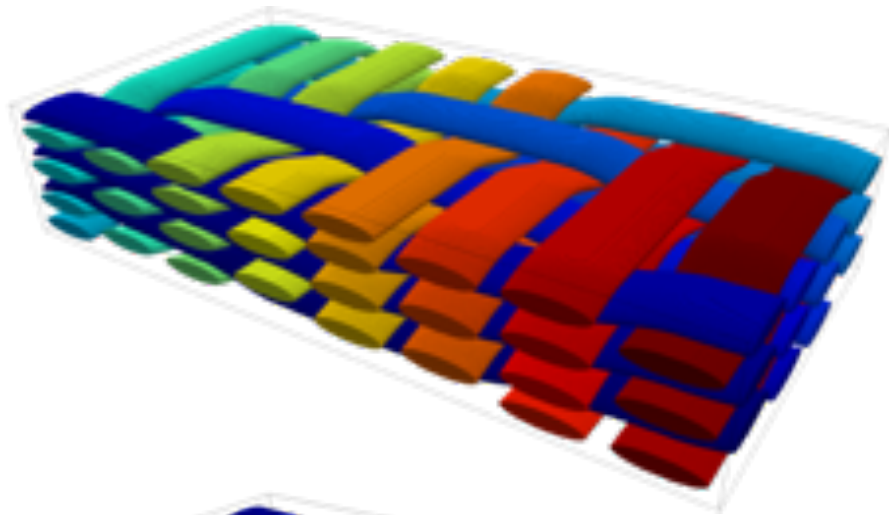




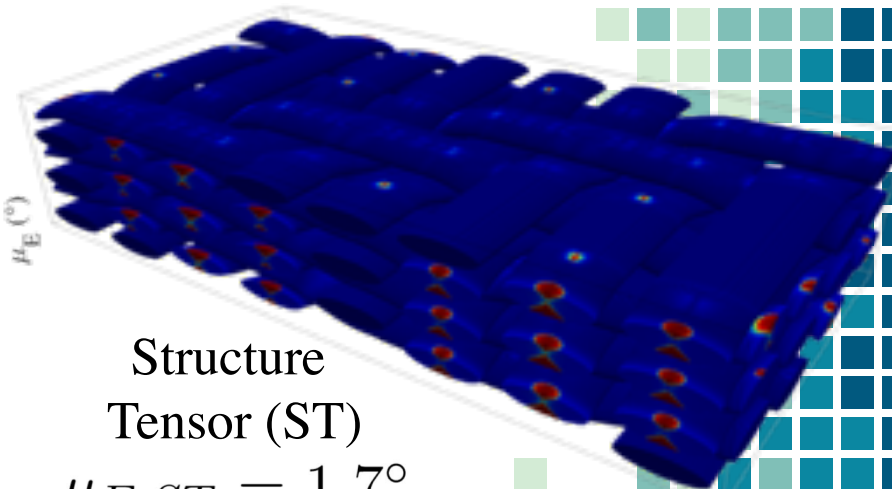
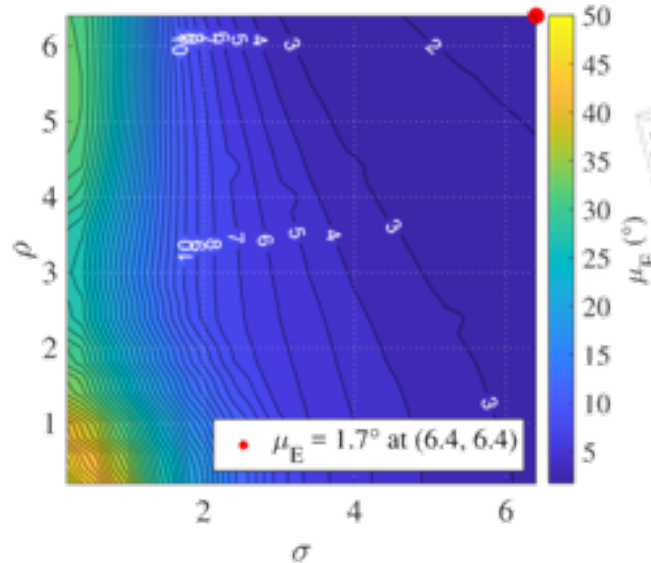
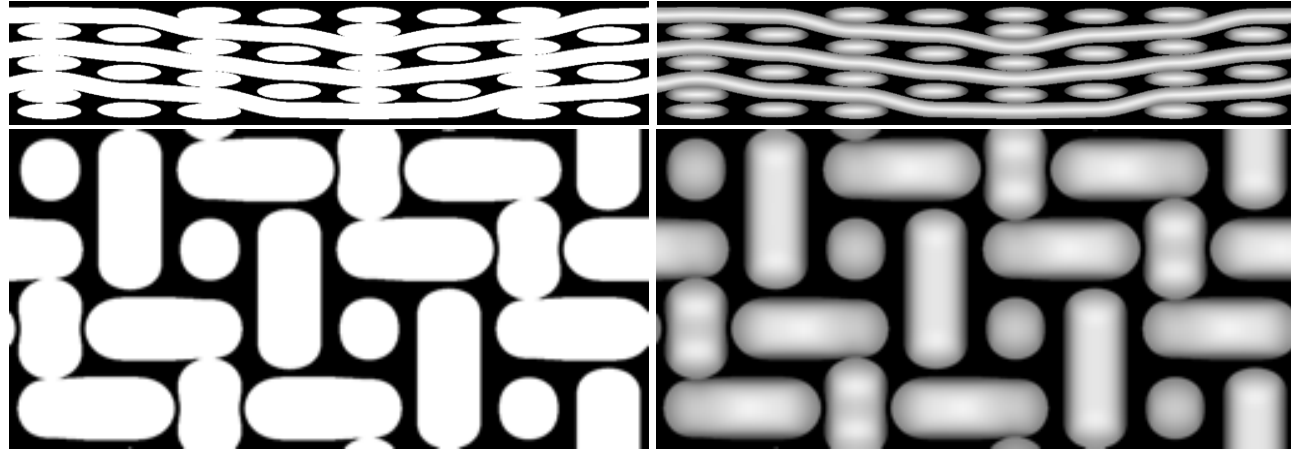


# Improved Workflow for Weave Orientation

Individual tow segmentation

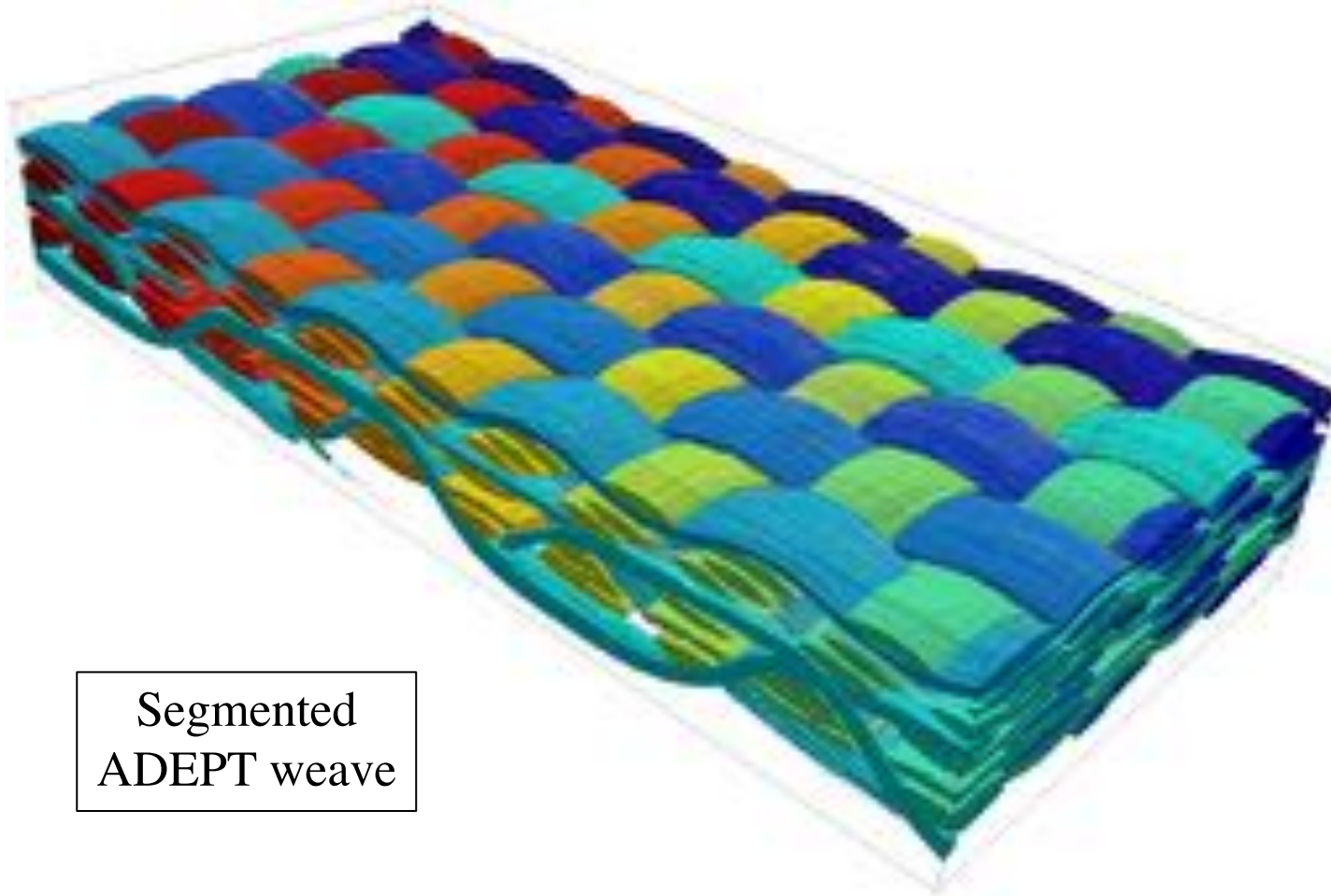


Mean Filtering



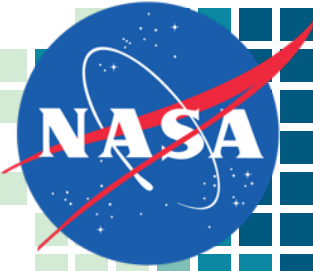
Structure Tensor (ST)  
 $\mu_{E,ST} = 1.7^\circ$

# Real Woven Sample\*<sup>1</sup>

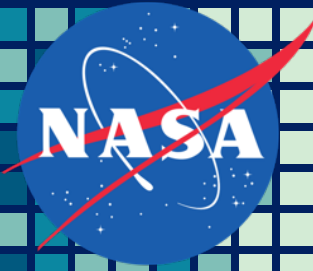


Segmented  
ADEPT weave

\*<sup>1</sup> J. M. L. MacNeil, D. M. Ushizima, F. Panerai, N. N. Mansour, H. S. Barnard, D. Y. Parkinson, Interactive volumetric segmentation for textile micro-tomography data using wavelets and nonlocal means, *Statistical Analysis and Data Mining: The ASA Data Science Journal* 12 (4) (2019) 338–353



# Summary



## 1. Ray Casting:

- Performs well on artificial straight fibers ( $\mu \sim 3 - 5^\circ$ ) and similar to other methods on binarized woven structures ( $\mu \sim 10 - 15^\circ$ ). Slight improvement in new workflow ( $\mu \sim 9^\circ$ )
- **Limitation:** affected by large fiber curvatures and computational expensive

## 2. Artificial Flux:

- Easy to use because independent on inputs. Performs similar to other methods on binarized weaves ( $\mu \sim 15^\circ$ ). Very accurate when using new workflow for woven materials ( $\mu \sim 1 - 3^\circ$ )
- **Limitation:** Performs poorly on artificial straight fibers due to regions not being in the path of heat flux through the material ( $\mu \sim 15 - 20^\circ$ )

## 3. Structure Tensor:

- Performs effectively on artificial straight fibers ( $\mu \sim 1 - 5^\circ$ ) and similar to other methods on binarized weaves ( $\mu \sim 20^\circ$ ). Very accurate when using new workflow for woven materials ( $\mu \sim 1 - 2^\circ$ )
- **Limitation:** hard to define optimal window a priori. For high resolutions, window must be sufficiently large, which can be very expensive